PRAMANA
— journal of
physics

Vol. 77, No. 1
July 2011
pp. 3–18

Hydrodynamic stability and stellar oscillations

H M ANTIA
Department of Astronomy and Astrophysics, Tata Institute of Fundamental Research,
Homi Bhabha Road, Mumbai 400 005, India
E-mail: antia@astro.tifr.res.in

Abstract. Chandrasekhar's monograph on *Hydrodynamic and hydromagnetic stability*, published in 1961, is a standard reference on linear stability theory. It gives a detailed account of stability of fluid flow in a variety of circumstances, including convection, stability of Couette flow, Rayleigh–Taylor instability, Kelvin–Helmholtz instability as well as the Jean's instability for star formation. In most cases he has extended these studies to include effects of rotation and magnetic field. In a later paper he has given a variational formulation for equations of non-radial stellar oscillations. This forms the basis for helioseismic inversion techniques as well as extension to include the effect of rotation, magnetic field and other large-scale flows using a perturbation treatment.

Keywords. Hydrodynamics; magnetohydrodynamics; helioseismology.

PACS Nos 95.30.Lz; 95.30.Qd; 96.60.Ly

1. Introduction

Chandra's monograph on *Hydrodynamic and hydromagnetic stability* published in 1961 [1] is the thickest and the most cited of the six monographs that he wrote. A search on the Astrophysics Data System shows about 2500 citations to this monograph and what is remarkable is that the number of citations during a year is steadily increasing, with about 140 citations recorded during 2010. This shows that this book is still the basic reference for a variety of stability problems in fluid mechanics. The first chapter of the book gives the basic concepts where the basic equations are derived. The next six chapters which form the bulk of the book are devoted to convection, or the thermal instability of a layer of fluid heated from below. The next three chapters are devoted to the stability of Couette flow, which is the flow between two rotating cylinders. The next two chapters are devoted to the stability of superposed fluids, one on Rayleigh–Taylor instability and the other on the Kelvin–Helmholtz instability. The next chapter is on stability of jets and cylinders. The final problem that is considered in this book is the gravitational instability, which is a generalization of Jean's criterion to situations with rotation and magnetic field. The final chapter of the book deals with a general variational principle.

Apart from this Monograph, an important related paper of Chandra is *A general variational principle covering the radial and the non-radial oscillations of gaseous masses*, which appeared in the *Astrophysical Journal* in 1964 [2]. This paper has played a

fundamental role in the study of stellar oscillations. These two works of Chandra and their impact on astrophysical research will be considered in this talk.

2. Convection

The problem of convection, or the stability of a fluid layer heated from below had been extensively studied both theoretically [3] and in laboratory experiments. Bénard [4] conducted a series of experiments to study convection in a thin layer of fluid, whose horizontal extent is much larger than the thickness in vertical direction, the direction in which gravity is acting. It is well known that as the layer is heated from below, initially there is no fluid motion as the required heat is transmitted by conduction. As the temperature gradient across the fluid layer is increased, at some stage convection sets in, where a part of the heat is transmitted through fluid motion. In this case hot fluid from below rises upward and mixes with the surrounding fluid, thus transmitting heat and in return a colder stream of fluid flows down, forming a convective cell. Such cellular patterns were seen by Bénard and others in their experiments. Chandra's monograph has many pictures from these experiments, and he has tried to explain the observed patterns.

Chandra's treatment is based on the linear stability analysis and further he used Boussinesq approximation, which essentially treats the fluid as incompressible. Thus this analysis is more suitable for laboratory experiments which mostly deal with liquids. Stellar convection zones can hardly be assumed to be incompressible or thin. The assumption of incompressibility filters out the acoustic waves, which simplifies the problem significantly. But at the same time if the fluid is totally incompressible, i.e., density is constant everywhere, there can be no buoyancy forces and hence no convection. Boussinesq approximation addresses this problem by requiring that although density, ρ, is independent of pressure, it weakly depends on temperature, T, through the coefficient of volume expansion, α, which is generally small for liquids in laboratory. Thus the density is written as

$$\rho = \rho_0 [1 - \alpha(T - T_0)]. \tag{1}$$

But since the density variation across the thin layer is small, this variation is neglected, except in the buoyancy term, which is written as

$$\delta\rho\mathbf{g} = -\alpha\rho_0\delta T\mathbf{g}, \tag{2}$$

where $\mathbf{g}$ is the acceleration due to gravity, which is assumed to be constant and acting along the z-axis. With these approximations the coefficients in the linearized equations for perturbations about the equilibrium state are constants and the x, y, t dependence of the solution can be written in the form:

$$\exp\bigl(i(k_x x + k_y y) + pt\bigr), \tag{3}$$

where $i = \sqrt{-1}$ and k_x and k_y are the wavenumbers along the x and y directions, respectively. Because of symmetry, only the magnitude of total horizontal wavenumber, $k = \sqrt{k_x^2 + k_y^2}$, is relevant.

The resulting equations are written in a dimensionless form using d, the height of the fluid layer as the unit of length and d^2/ν as the unit of time, where ν is the kinematic viscosity. The resulting equations depend on some dimensionless constants, i.e., the Rayleigh number,

$$R = \frac{g\alpha\beta d^4}{\kappa\nu}, \tag{4}$$

the Prandtl number $\mathcal{P} = \nu/\kappa$, and the dimensionless wavenumber $a = kd$ and the growth rate $\sigma = pd^2/\nu$. Here, κ is the thermal diffusivity and β is the temperature gradient across the fluid layer, which is assumed to be constant. The linearized equations along with appropriate boundary conditions form an eigenvalue problem and a non-trivial solution exists for some discrete values of the eigenvalue σ. This gives the dispersion relation $\sigma(R, \mathcal{P}, a)$. The wavenumber a defines the length-scale of perturbations and for stability we require $\text{Real}(\sigma) < 0$ for all permissible values of a. This ensures that perturbations at all length-scales are stable. Chandra has done extensive analysis of this equation for different boundary conditions to analyse stability.

Since σ is a continuous function of its arguments, the transition to instability occurs when $\text{Real}(\sigma) = 0$, which yields two possibilities, $\sigma = 0$ or σ is purely imaginary, i.e., the solution is either stationary or purely oscillatory in time. When σ is real, the state of marginal stability is given by $\sigma = 0$, which means the resulting solution is independent of time, and the state is also referred to as stationary convection. In this case the principle of the exchange of stability is said to be applicable. Chandra has shown that in the absence of rotation and magnetic field the transition to instability happens through this route. The second possibility of σ being purely imaginary can occur in the presence of rotation or magnetic field and in that case the transition to instability can happen through oscillatory modes, which is referred to as overstability. This term was coined by Ledoux and implies that in this case, if a fluid element is displaced from its equilibrium position, it will come back to this position with larger velocity and the amplitude of oscillation keeps increasing with time.

For the case without rotation and magnetic field, the transition to instability occurs through stationary convection, $\sigma = 0$, and in this case the equations are independent of the Prandtl number. Thus, the condition $\sigma = 0$ gives the Rayleigh number as a function of the dimensionless wavenumber, $R(a)$. The function $R(a)$ gives the value of Rayleigh number at which the mode with a given wavenumber a becomes unstable. Since for $R \to 0$, i.e., for large viscosity the fluid layer is stable, the instability occurs when $R > R(a)$ for a given a. Minimizing this function with respect to a gives the critical Rayleigh number, R_c. If the Rayleigh number of the fluid layer is less than this critical value, there cannot be any transition to instability and the fluid layer is stable. For instability R has to be greater than R_c and in that case modes with wavenumber a for which $R(a) \leq R$ are unstable. Further, the value of a for which $R(a)$ is minimum gives the length-scale of modes that would be excited when R just exceeds the critical value. In the critical case $R = R_c$ only the mode with this wavenumber will survive. This essentially determines the length-scale observed in experiments at the onset of convection. In these experiments, typically the temperature gradient is increased slowly till convection sets in and the critical value of the Rayleigh number and the resulting pattern of convective cells is studied. Although the linear stability analysis does not give any information about the shape of the resulting

convective cellular pattern, Chandra has analysed various possibilities and compared them with experimentally observed pattern. He has also compared the theoretically obtained critical Rayleigh number with experimentally obtained values.

Rotation introduces additional forces and the simplest case arises when the rotation axis is parallel to gravitational force. In the presence of rotation the equations involve another dimensionless constant, the Taylor number

$$T = \frac{4\Omega^2 d^4}{\nu^2} \,, \tag{5}$$

where Ω is the rotation frequency. Once again, the stability can be analysed by considering the dispersion relation and there are two possibilities for the onset of instability. If the onset of instability occurs through stationary convection ($\sigma = 0$), then once again the equations are independent of the Prandtl number and the condition $\sigma = 0$ yields $R(a, T)$. Finding the minimum with respect to a gives the critical Rayleigh number R_c, which in this case is also a function of T, and its value is found to increase with T. For $T = 0$, the non-rotating case is recovered. As before, the fluid layer is stable if $R < R_c$ for a given T. The increase in R_c with T implies that rotation tends to stabilize the fluid against convection.

However, in the presence of rotation there is the second possibility that the onset of instability occurs through overstability, or oscillatory instability. This is possible only when $\mathcal{P} < 1$. Once again the condition that σ is purely imaginary gives the required conditions. In this case there are two equations, one for the real part and the other for the imaginary part of the equation. The additional equation can be used to eliminate the imaginary part of σ which is the frequency of oscillatory mode, giving a relation between R, $\mathcal{P}$, T and a. For a given value of $\mathcal{P}$, T the value of R can be minimized with respect to a to get the critical value R_c. If this critical value happens to be less than that for stationary convection, then the onset of instability will occur through overstability, otherwise stationary convection will prevail. It should be noted that for transition to instability through stationary convection, R_c is independent of $\mathcal{P}$. Thus, to analyse the stability in the presence of rotation, Chandra has plotted R_c as a function of T for the required value of $\mathcal{P}$ for the onset of instability through overstability. On the same plot the curve for stationary convection is also shown. For small values of T the value of R_c is smaller for stationary convection as compared to that for overstability and the transition to instability occurs through stationary convection. As T increases the two curves intersect and for larger values of T the onset of instability occurs through overstability. The point of intersection gives the critical value of T, which separates the region where instability arises through stationary convection from that where it arises through overstability.

Similar results were obtained with magnetic field. Chandra has also considered the situation where rotation axis does not coincide with gravity, as well as situations including both rotation and magnetic field. Chandra's work has been extended to a nonlinear case where the Rayleigh number is marginally above the critical value. This can give information about the shape of convective cells. Another extension is to compressible fluid, which is more relevant for stellar convection. In this case the density stratification needs to be included and it is not possible to solve the equations analytically. Numerical solution of these equations does not give the same level of insight as that obtained by Chandra. The presence of acoustic modes in compressible fluids is an added complication.

With enhanced computing power it is now possible to do fully nonlinear calculations for a fluid in a box. These calculations cannot yet account for all relevant length-scales of turbulence in stellar convection zones where Rayleigh number exceeds the critical value by several orders of magnitude. Nevertheless, such calculations have been very successful in understanding solar granulation [5–7]. Solar granulation [8] is the observed manifestation of convection near the solar surface. The solar granules are of irregular shape with a length-scale of about 2000 km, with brighter regions representing the hotter fluid coming from below and the darker regions showing the cooler fluid flowing downward. The numerical simulations have been performed in a box of limited size, but they show a pattern which is similar to the observed granulation. The numerical simulations have also successfully matched the spectral line profiles for many spectral lines. While these simulations have been successful in explaining granulation, the success is limited in other aspects. The most notable failure of simulations has been the prediction that rotation rate should be nearly constant on cylinders, which was not confirmed by helioseismically inferred rotation rate in the solar interior (see §5.2). Similarly, the use of these simulations to determine abundances of heavy elements has lowered the heavy element abundances significantly [9]. These reduced abundances are not consistent with helioseismology [10]. However, independent numerical simulations [11] have found higher abundances, which may be consistent with helioseismology. This issue still needs to be studied.

3. Impact of Chandra's monograph

As mentioned earlier, Chandra's monograph has about 2500 citations, which is a measure of its impact. These papers cover a wide range of subjects in astrophysics and some of them are even beyond astronomy. Some of these papers which cite the monograph in turn have made a large impact. To get an idea of the range of topics covered by these, we describe below the top six papers among these whose citations range from about 2600 to 470.

1. *Pattern formation outside of equilibrium*: Cross and Hohenberg (1993) [12]
   This paper discusses pattern formation in Bénard convection when the Rayleigh number exceeds the critical value ($R > R_c$) and in Couette flow, which is a direct extension of Chandra's work. They have obtained the 'amplitude equations', to describe the growth of perturbation when the system is marginally unstable.
2. *Theory of extragalactic radio sources*: Begelman, Blandford and Rees (1984) [13]
   Powerful extragalactic radio sources typically consist of two extended regions, each linked by a jet to a central compact radio source located in the nucleus of the associated galaxy. This paper discusses collimation of these jets, including the role of the Kelvin–Helmholtz instability in determining the properties of these jets.
3. *Instability and pattern formation in crystal growth*: Langer (1980) [14]
   This is an example of application of stability analysis beyond astronomy.
4. *The dynamical state of the interstellar gas and field*: Parker (1966) [15]
   In this paper Rayleigh–Taylor instability in the presence of galactic magnetic field is invoked to explain the observed tendency of interstellar gas to be confined in discrete clouds.
5. *Gas dynamics of semidetached binaries*: Lubow and Shu (1975) [16]

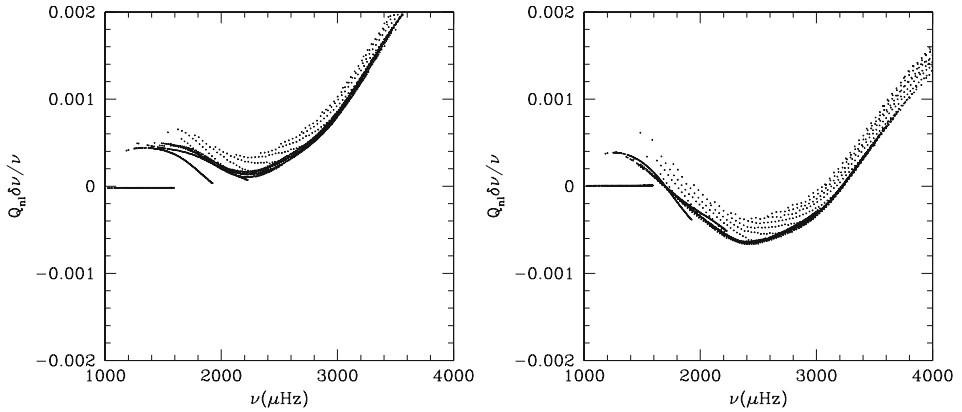

Figure 1. Relative frequency difference between two solar models and the observed frequencies from the MDI instrument is shown as a function of frequencies. The frequency differences are scaled by mode inertia. The left panel shows the differences for the model using the mixing length theory, while the right panel shows the same for the model using the prescription of Canuto and Mazzitelli [17].

This paper considers the role of Kelvin–Helmholtz instability to describe the dynamics of mass transfer from the contact component in a binary system to the detached companion star.

6. *Stellar turbulent convection* – A new model and application: Canuto and Mazzitelli (1991) [17]
This paper gives a prescription to calculate convective flux in stellar convection zones. They use some treatment of turbulence to calculate the distribution of convective cells in stellar convection zone and use it to calculate the net convective flux, which can substitute the expression obtained from the mixing length theory, normally used for this purpose. Helioseismic data show that a solar model constructed using this prescription is in better agreement with observations as compared to the one using mixing length theory [18]. Figure 1 compares the frequency difference between a pair of solar models and the observed frequencies from MDI instrument [19]. One of the models is constructed using the mixing length theory and the other using the prescription of Canuto and Mazzitelli. It is clear that frequency differences are significantly less for the latter.

4. Nonradial oscillations of stars

Chandrasekhar [2] showed that the equations of stellar oscillations with simple boundary conditions form a Hermitian eigenvalue problem and hence follow a variational formulation:

$$\sigma^2 \int_V \rho|\xi|^2 \,\mathrm{d}\mathbf{x} = \int_V \left[\gamma p(\nabla\cdot\xi)^2 + \frac{2}{r}\frac{\mathrm{d}p}{\mathrm{d}r}(\mathbf{x}\cdot\xi)\nabla\cdot\xi\right] \mathrm{d}\mathbf{x} + \int_V \frac{(\mathbf{x}\cdot\xi)^2}{r^2\rho}\frac{\mathrm{d}\rho}{\mathrm{d}r}\frac{\mathrm{d}p}{\mathrm{d}r}\,\mathrm{d}\mathbf{x} - G\int_V\int_V \frac{(\nabla\cdot\rho\xi)_x(\nabla\cdot\rho\xi)_{x'}}{|\mathbf{x}-\mathbf{x}'|}\,\mathrm{d}\mathbf{x}\,\mathrm{d}\mathbf{x}'. \quad (6)$$

Here, ξ is the displacement from equilibrium position, σ is the frequency of oscillatory mode, p is the pressure, γ is the adiabatic index and G is the gravitational constant. These equations were used to obtain the normal modes of oscillations in terms of vector spherical harmonics:

$$\xi_r = \frac{\psi(r)}{r^2} Y_\ell^m(\theta, \phi), \tag{7}$$

$$\xi_\theta = \frac{1}{\ell(\ell+1)r} \frac{\mathrm{d}\chi(r)}{\mathrm{d}r} \frac{\partial Y_\ell^m(\theta, \phi)}{\partial \theta}, \tag{8}$$

$$\xi_\phi = \frac{1}{\ell(\ell+1)r \sin\theta} \frac{\mathrm{d}\chi(r)}{\mathrm{d}r} \frac{\partial Y_\ell^m(\theta, \phi)}{\partial \phi}. \tag{9}$$

Here, $\psi(r)$ specifies the radial dependence of the radial component of displacement, while $\chi(r)$ specifies the radial dependence of the horizontal component of displacement. These two functions $\psi(r)$, $\chi(r)$ and the eigenfrequency σ are calculated by applying the variational principle. The stellar oscillation modes can be identified by three quantum numbers, i.e. the degree ℓ and azimuthal order m defining the spherical harmonic and the radial order n, which determines the number of nodes in the radial part $\psi(r)$ of the eigenfunction.

The formulation for radial oscillations ($\chi(r) = 0, \ell = 0$) was also obtained. Chandra also obtained the so-called Kelvin mode, or the f-mode using $\psi = \chi = r^{\ell+1}$ to get

$$\sigma^2 = \frac{2\ell(\ell-1)}{2\ell+1} G \frac{\int_0^R \rho r^{2\ell-3} M(r)\, \mathrm{d}r}{\int_0^R \rho r^{2\ell}\, \mathrm{d}r} \approx \ell \frac{GM}{R^3} = gk \qquad (\ell \to \infty). \tag{10}$$

Here the last approximation is valid only for large ℓ. These modes are essentially surface gravity modes and their frequency is largely independent of stratification in the stellar interior, depending mainly on the surface gravity. The frequencies of f-modes have been used to estimate the solar radius [20,21]. The seismically determined solar radius is found to be about 200–300 km less than the standard value. Some of the difference is due to different definitions of solar surface used in the two cases.

Chandra's paper has over 100 citations covering a wide range of topics in astrophysics. Most of the citations are from papers in helioseismology as the variational principle forms the basis for the study of stellar oscillations. The three most prominent papers which have got about 240 citations each are

1. *On formation of close binaries by two-body tidal capture*: Press and Teukolsky (1977) [22]
   This paper used the mechanism of Fabian *et al* [23] where two stars in hyperbolic orbit have a close encounter, which leads to an elliptic orbit when sufficient energy is transferred from orbital motion to nonradial oscillations in these stars. This mechanism was proposed for the formation of X-ray binaries in globular clusters. They formulated the problem as a forced oscillator with tidal forces forming the forcing term:

$$\left(\mathcal{L} - \rho\omega^2\right) \xi = \rho \nabla U. \tag{11}$$

Here, $\mathcal{L}\xi = \rho\omega^2\xi$ defines the eigenvalue problem for nonradial oscillations in stars, where ω is the frequency of oscillation mode. The operator $\mathcal{L}$ can be obtained from the variational principle. By expanding the tidal forcing on the right-hand side in terms of eigenfunctions, they obtained the amplitude of normal modes that are excited, which in turn gives an estimate of the energy transfer.

2. *Rapidly rotating neutron star models*: Friedman, Ipser and Parker (1986) [24]
   This paper deals with the structure of rapidly rotating relativistic models for neutron stars with various nuclear matter equations of state. They obtained upper limit on rotation rate for different models by considering the stability of models.
3. *On the stability of differentially rotating bodies*: Lynden-Bell and Ostriker (1967) [25]
   This paper generalized the variational principle to a differentially rotating self-gravitating body. Clement [26] had generalized the variational principle to uniformly rotating star. The analysis for differential rotation is significantly more complicated than for uniform rotation, which only needs additional forces in a rotating frame. For differential rotation, even in a rotating frame the fluid is not at rest and hence the equilibrium state is not static. This formulation could be used to study stability of differentially rotating stars.

5. Application of variational principle to stellar oscillations

Variational formulation has been used to study the effect of small perturbations to basic spherically symmetric stellar model. The perturbations could be due to other forces, e.g., rotation or magnetic field or due to perturbation in the stellar models or due to truncation error in numerical calculation of frequencies. We can write the perturbed operator as $\mathcal{L}+\delta\mathcal{L}$ giving the eigenvalue problem

$$(\mathcal{L} + \delta\mathcal{L})\xi = \rho(\omega^2 + \delta\omega^2)\xi, \tag{12}$$

and in a degenerate perturbation theory we get

$$\delta\omega_\lambda^2 = \frac{\langle\xi_\lambda^*\delta\mathcal{L}\xi_\lambda\rangle}{\langle\xi_\lambda^*\rho\xi_\lambda\rangle}. \tag{13}$$

Here, λ labels the oscillation mode, which may be a combination of the three quantum number, n, ℓ, m mentioned earlier. This equation can be used to calculate the frequency shift due to the perturbation and forms the basis for a good deal of problems in helioseismology.

Since solar oscillation frequencies have been measured to a very high accuracy of about 1 part in 10^5, the solar model frequencies also need to be calculated to even better accuracy for proper comparison. The second-order finite difference approximation that is normally used to solve the eigenvalue problem does not give the required accuracy unless the number of mesh points is larger than 10,000, which is too large to handle in a stellar evolution code. Thus to get higher-order accuracy, the truncation error in this difference approximation is treated as a perturbation and the correction to the frequency calculated using the variational principle (eq. (13)). The corrected frequency has significantly less truncation error.

5.1 *Inversion for solar structure*

If we consider perturbation to a stellar model, the change can be expressed in terms of perturbation in the speed of sound and density, and applying the variational principle, we get

$$\frac{\delta\nu_{n\ell}}{\nu_{n\ell}} = \int_0^R \mathcal{K}^{n\ell}_{c^2,\rho}(r)\frac{\delta c^2}{c^2}(r)\,\mathrm{d}r + \int_0^R \mathcal{K}^{n\ell}_{\rho,c^2}(r)\frac{\delta\rho}{\rho}(r)\,\mathrm{d}r, \tag{14}$$

where c is the speed of sound and ρ is the density in a stellar model. Here, $\mathcal{K}^{n\ell}_{\rho,c^2}(r)$ and $\mathcal{K}^{n\ell}_{c^2,\rho}(r)$ are the kernels, which involve the stellar model as well as the eigenfunction for the concerned mode of oscillation. In this equation, δc^2, $\delta\rho$ and $\delta\nu_{n\ell}$ are respectively the differences in the squared sound speed, density and frequency between the two solar models. The actual equation for inversion includes one more term arising from the surface effects which is not shown in eq. (14). Equation (14) can be used to calculate the frequency differences between two solar models, by using the known δc^2 and $\delta\rho$ between these models. On the other hand, if the frequency difference for a large set of modes is known, it defines the inverse problem to determine δc^2 and $\delta\rho$ between these models. Similarly, by using the difference between observed frequencies of solar oscillations and that for a solar model, one can calculate δc^2 and $\delta\rho$ between the Sun and a solar model [27]. Because of the finite number of modes that are available, the inverse problem cannot give a unique profile, but by assuming that the differences are smooth in some sense it is possible to get a reasonable estimate for the speed of sound and density in the Sun. The inversion techniques have been extensively tested during the last two decades and there is a very good agreement between the results obtained by different techniques.

It can be shown that c, ρ along with the equation of hydrostatic equilibrium are enough to determine the solar model as far as frequencies are concerned. Pressure p and adiabatic index $\Gamma_1 = (\partial \ln p/\partial \ln \rho)_s = c^2\rho/p$ can be determined from c, ρ. Instead of c, ρ any other pair of independent variables can be used for inversion. Figure 2 shows the results of inversion using two solar models. It can be seen that the speed of sound in the solar model is within about 0.2% of that in the Sun, while density has somewhat larger differences. The largest difference arises just below the base of the convection zone and has been attributed to the lack of mixing below the convection zone in the standard solar model. The figure also shows the differences for a model which incorporates mixing below the base of the convection zone [29] and it is clear that this model is in better agreement in this region. The discrepancy in the near surface layers is due to error is solar radius which arises because of difficulty in modelling the surface layers. Most of this discrepancy can be eliminated by scaling the radius in the solar model appropriately.

The helioseismic inversions have provided severe constraints on solar models and there have been significant improvements in input physics since the seismic inversions were first performed. There has been a steady improvement in solar models over the last two decades. However, Asplund *et al* [30] calculated the abundances of oxygen and other heavy elements in the Sun using improved 3D atmospheric models based on numerical simulations to find that the abundances need to be significantly reduced. Solar models with reduced abundances are not consistent with seismic constraints [31,32]. Since then numerous attempts have been made to modify the solar models in a variety of ways, but none has succeeded in obtaining seismically consistent models using revised abundances [10]. With the revised

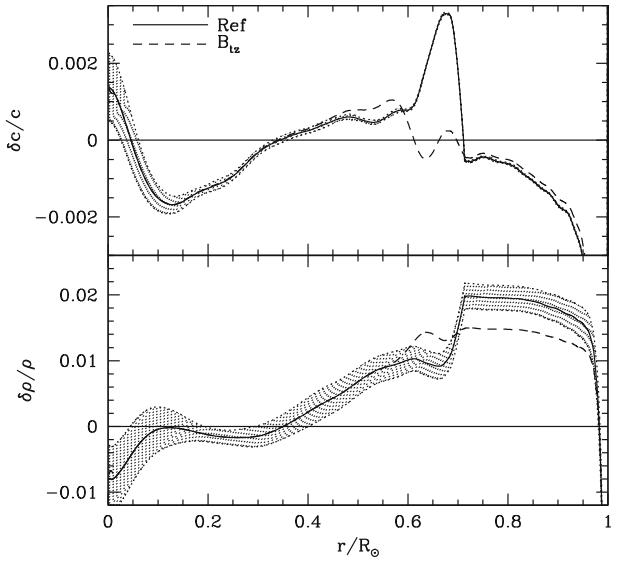

Figure 2. Relative difference in speed of sound (lower panel) and density (upper panel) between the Sun and two solar models. The inversions were done using data from the GONG project [28]. The solid lines show the result for a standard solar model, while the dashed line shows the result for a model with mixing in tachocline region [29]. For clarity, error bars are shown only for the standard model.

abundances the discrepancy in speed of sound increases to about 1.5% and that in density to about 10% [10]. As mentioned earlier, there is some discrepancy between abundances calculated using different techniques, including different 3D numerical simulations and more effort is needed to resolve this discrepancy.

5.2 *Inversion for rotation rate*

Apart from solar structure, it is possible to study the rotation rate in the solar interior using observed frequencies of solar oscillations. In the absence of rotation, the frequencies are independent of the azimuthal order m, and rotation lifts the degeneracy giving rise to frequency splittings, which can be used to study the rotation rate in the solar interior. Ritzwoller and Lavely [33] treated rotation as a perturbation on spherically symmetric stellar model to calculate the first-order effect of rotation, arising from the Coriolis force which gives a perturbation to the operator $\mathcal{L}$,

$$\delta\mathcal{L} = 2i\omega\rho\mathbf{v}_{\rm rot}\cdot\nabla\xi, \tag{15}$$

which can be used to calculate the frequency splitting due to rotation. The frequency splitting can be expressed as

$$\nu_{n,\ell,m} = \nu_{n,\ell} + \sum_{j=1}^{M} a_j^{(n,\ell)} P_j(m), \tag{16}$$

where $a_j^{(n,\ell)}$ are the splitting coefficients and $P_j(m)$ are orthogonal polynomials of degree j in the azimuthal order m. The number of splitting coefficients, M, in the summation is less than 2ℓ. Similarly, the rotation velocity is decomposed as

$$v_\phi(r,\theta) = -\sum_{j=1}^{M} w_{2j-1}(r)\frac{\partial Y_{2j-1}^0}{\partial\theta}\ . \tag{17}$$

With this decomposition, using the variational principle the splitting coefficients are given by

$$a_j^{(n,\ell)} = \int_0^R w_j(r)\mathcal{K}_j^{(n,\ell)}(r)r^2\ \mathrm{d}r \tag{18}$$

$$= \int_0^R\int_{-1}^1 \Omega(r,\theta)\mathcal{K}_j^{(n,\ell)}(r,\theta)\ \mathrm{d}r\ \mathrm{d}\cos\theta. \tag{19}$$

Here, $\Omega(r,\theta)$ is the rotation rate and $\mathcal{K}_j^{(n,\ell)}$ are the kernels and either of these forms can be used. This equation can be used to calculate the splitting coefficients for a specified rotation rate profile. Alternately, if the splitting coefficients are known for a large number of modes, this equation can be used for inversion of rotation rate from the observed splitting coefficients [34].

The splitting coefficients are sensitive only to the north–south symmetric component of rotation rate and hence that is the only component that can be determined. Observations at the solar surface show that the north–south antisymmetric component of rotation is fairly small and has not been determined reliably. Figure 3 shows the result of such an inversion using MDI data. It is clear that there is a strong shear layer near the surface where the rotation rate increases with depth. Further, the known differential rotation at

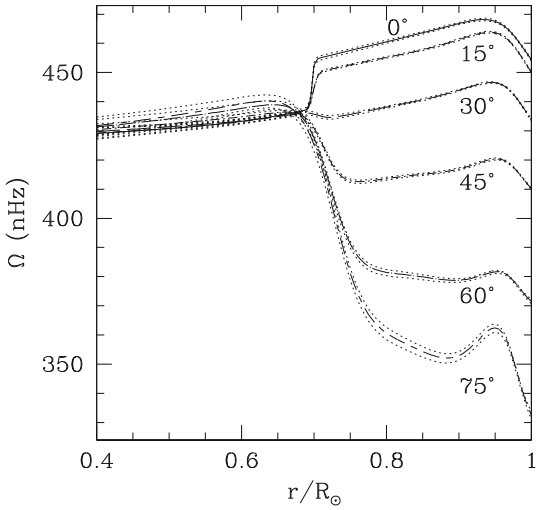

Figure 3. Rotation rate in the solar interior as inferred by inversion of Michelson Doppler image (MDI) data is shown as a function of radial distance for a few selected latitudes as marked in the figure. The dotted lines show the 1σ error limits in each case.

the solar surface persists through the convection zone, while below the convection zone, the rotation rate is almost independent of latitude. The narrow transition region around the base of the convection zone is referred to as the tachocline [35] and it is still not clear how this layer is formed. The tachocline is generally believed to be the region where the solar dynamo operates. Further, the inferred rotation rate is clearly inconsistent with the theoretical predictions of constant rotation on cylinders.

Once the rotation rate is known in the solar interior, it is possible to calculate the global quantities like the angular momentum and kinetic energy. It is also possible to calculate the oblateness induced by rotation and the resulting gravitational quadrupole moment [36]

$$\text{Angular momentum: } H = (190.0 \pm 1.5) \times 10^{46} \text{ g cm}^2 \text{ s}^{-1}, \tag{20}$$

$$\text{Kinetic energy: } T = (253.4 \pm 7.2) \times 10^{40} \text{ g cm}^2 \text{ s}^{-2}, \tag{21}$$

$$\text{Quadrupole moment: } J_2 = (2.18 \pm 0.06) \times 10^{-7}. \tag{22}$$

The quadrupole moment plays a role in the test of general relativity using the observed precession of perihelion of Mercury. If the Sun has significant departure from spherical symmetry, then it will also give some contribution to the precession from purely Newtonian effects, thus causing a discrepancy between the relativistic prediction and the observed rate. There were some claims that solar core is rotating much faster, thus giving some contribution to the precession [37]. However, the helioseismically determined rotation rate does not show any increase in the core and the resulting J_2 will cause precession of perihelion of Mercury by $0.03''$ per century, which is within the error estimates, thus validating the test of general relativity.

5.3 *Effect of magnetic field on stellar oscillations*

Gough and Thompson [38] extended the study to include second-order effect of rotation and magnetic field using the equation

$$(\mathcal{L} - \rho\omega^2)\xi = \omega\mathcal{M}\xi + \mathcal{N}\xi + \mathcal{B}\xi, \tag{23}$$

where $\mathcal{M}$ is the term due to Coriolis force which is used to calculate the effect of rotation (eq. (15)), $\mathcal{N}$ is the contribution from centrifugal force and $\mathcal{B}$ includes the contribution from magnetic field. The second-order effects contribute to the even order splitting coefficients and can be separated from first-order effect of rotation, which contribute only to the odd order splitting coefficients. They also calculated the effect of departure from spherical symmetry in the equilibrium model due to rotation or magnetic field. The second-order effect of rotation arises from the centrifugal force term and the distortion from spherical symmetry as well as from the first-order perturbations to the eigenfunctions, while magnetic field does not have any first-order contribution to the frequencies of stellar oscillations.

The magnetic field was considered to be axisymmetric, either toroidal

$$\mathbf{B} = \left[0, 0, a(r)\frac{\mathrm{d}}{\mathrm{d}\theta}P_k(\cos\theta)\right], \tag{24}$$

or poloidal

$$\mathbf{B} = \left[k(k+1)\frac{b(r)}{r^2}P_k(\cos\theta), \frac{1}{r}\frac{\mathrm{d}b}{\mathrm{d}r}\frac{\mathrm{d}}{\mathrm{d}\theta}P_k(\cos\theta), 0\right]. \tag{25}$$

Here $P_k(\cos\theta)$ is the Legendre polynomial of degree k. The radial dependence of the toroidal field is taken to be [39]

$$a(r) = \begin{cases} \sqrt{8\pi p\beta_0}(1 - (\frac{r-r_0}{d})^2) & \text{if } |r - r_0| \le d, \\ 0 & \text{otherwise,} \end{cases} \tag{26}$$

where p is the pressure and β_0 is a constant which gives the ratio of magnetic to gas pressure. Here the magnetic field is confined in a layer of thickness $2d$ around $r = r_0$ and the symmetry axis of magnetic field is assumed to coincide with the rotation axis. For $k = 2$, $\beta_0 = 10^{-4}$, $r_0 = 0.713R_\odot$, $d = 0.01R_\odot$, the splitting coefficients as a function of lower turning point of the modes are shown in figure 4. The turning point is given by the layer where $\left(\ell(\ell+1)c^2(r_t)/r_t^2\right) = \omega^2$. The acoustic modes are typically trapped in a region $R_\odot \ge r \ge r_t$. The upper turning point for the modes is close to the solar surface for the observed modes of solar oscillations. The figure shows a characteristic signature of splitting coefficients arising from a localized toroidal field near the base of the convection zone. Since such a pattern is not seen in the observed data we can only put an upper limit on the magnetic field in this region [39]. These limits are not very useful for constraining dynamo models which assume a toroidal field in this region, since the field in dynamo model is assumed to be concentrated in flux tubes and we need to account for the filling factor before comparing with the seismic limits. With a reasonable filling factor and currently accepted field strength in the tachocline region, the splitting coefficients are too small to be detected.

Since the even splitting coefficients are fairly small, it is not yet possible to invert them for the magnetic field. The rotation rate can be inferred from the odd splitting coefficients and the inferred rotation rate can be used to calculate second-order contribution from rotation, which should be subtracted from the observed splitting coefficients to get the residual contribution, which may be due to magnetic field or other departures from spherical symmetry. It is not possible to separate these two contributions. Assuming that the residual coefficients are entirely due to the large-scale magnetic field, it is possible to obtain some

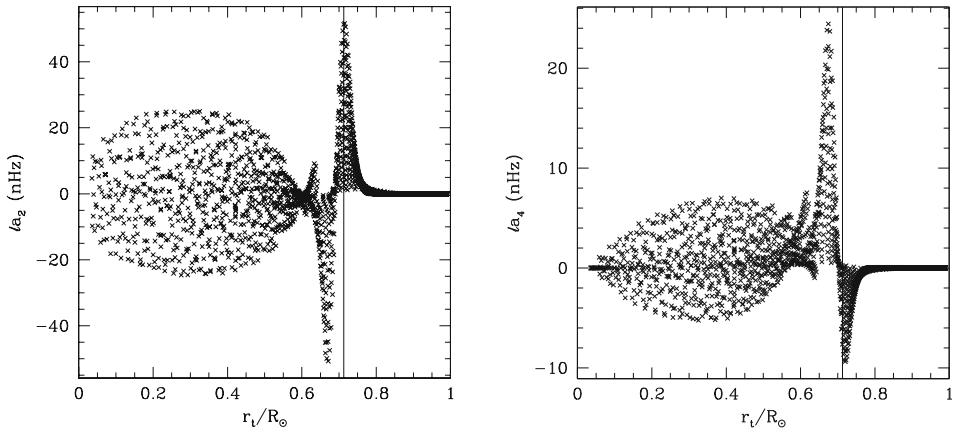

Figure 4. Splitting coefficients, a_2, a_4 due to a toroidal magnetic field with $k = 2$, $\beta_0 = 10^{-4}$, $r_0 = 0.713R_\odot$ and $d = 0.01R_\odot$ are shown as a function of the lower turning point of the modes.

estimates of magnetic field [40]. These studies show that most of the contribution to even splitting coefficients arise from magnetic field near the solar surface, typically within 1% of the solar radius. There is very little signature of magnetic field in deeper layers. Further, the near-surface magnetic field is found to vary with time in phase with solar activity.

5.4 *Effect of meridional flows on stellar oscillations*

In general, the first-order contribution to frequency shift from meridional flow, or the north–south antisymmetric component of rotation vanishes in the degenerate perturbation theory and one has to use the quasi-degenerate perturbation theory [41] to calculate these contributions. In this case the eigenfunction is written as the sum of eigenfunctions of spherically symmetric model with close frequencies

$$\xi'_{\mathbf{k}} = \sum_{k'} a_{k'} \xi_{\mathbf{k}'}, \tag{27}$$

where the summation is taken over a set of modes with frequencies close to the mode being perturbed. The equation is given by

$$(\mathcal{L} - \rho\omega_k'^2)\xi'_{\mathbf{k}} + \delta\mathcal{L}\xi'_{\mathbf{k}} = 0. \tag{28}$$

By taking the scalar product with ξ_j, it gives a set of equations:

$$\sum_{k'} a_{k'} \left[H_{jk'} + \delta_{jk'}(\omega_{k'}^2 - \omega_k^2)\right] = a_j(\omega_k'^2 - \omega_k^2), \tag{29}$$

where $H_{jk} = \langle \xi_{\mathbf{j}}^* \delta\mathcal{L}\xi_{\mathbf{k}} \rangle$. This system of equations constitute an eigenvalue problem, which can be solved to calculate the frequency shifts for the mode.

The axisymmetric meridional velocity is assumed to be of the form

$$\mathbf{v_s}(r,\theta) = \left[u_s(r)P_s(\cos\theta), v_s(r)\frac{\mathrm{d}}{\mathrm{d}\theta}P_s(\cos\theta), 0\right], \tag{30}$$

$$v_s(r) = \frac{1}{\rho r}\frac{\mathrm{d}}{\mathrm{d}r}\left(\frac{\rho r^2 u_s(r)}{s(s+1)}\right), \tag{31}$$

$$u_s(r) = \begin{cases} u_0 \frac{4(R-r)(r-r_b)}{(R-r_b)^2} & \text{if } r_b \le r \le R, \\ 0 & \text{otherwise.} \end{cases} \tag{32}$$

Here, u_s is the radial component of velocity, while v_s is the horizontal component in the north–south direction, $P_s(\cos\theta)$ is the Legendre polynomial of degree s. Here the meridional velocity is assumed to be confined in the region $r_b \le r \le R$. The upper limit is taken to be the solar surface, while the lower limit of the region where the meridional flow persists is not known and it is generally assumed that the meridional flow penetrates to the base of the convection zone or a little below it. With these meridional flow field, it is possible to compute the splitting coefficients, as well as the shift in the mean frequencies, but the value is found to be very small, of the order of a few nHz [42]. Although, in principle, these may be detectable, there is no characteristic signature of the resulting frequency shift and it is not possible to distinguish between contribution of meridional flow and those from near surface magnetic field. Further, the calculated splitting coefficients are not sensitive to

r_b the depth to which meridional flow penetrates. This depth plays an important role in the flux transport dynamo models.

From the above discussion it is clear that the variational principle given by Chandrasekhar has played a fundamental role in helioseismology.

Acknowledgements

Most of the results quoted in this work and the figures shown were obtained using data from the MDI and GONG projects. Michelson Doppler imager (MDI) is an instrument on board the Solar and Heliospheric Observatory (SOHO). SOHO is a project of international cooperation between ESA and NASA. MDI is supported by NASA grant NAG5-8878 to Stanford University. The Global Oscillation Network Group (GONG) program is managed by the National Solar Observatory, which is operated by AURA, Inc. under a cooperative agreement with the National Science Foundation. The data were acquired by instruments operated by the Big Bear Solar Observatory, High Altitude Observatory, Learmonth Solar Observatory, Udaipur Solar Observatory, Instituto de Astrofisica de Canarias, and Cerro Tololo Interamerican Observatory.

References

[1] S Chandrasekhar, *Hydrodynamic and hydromagnetic stability* (Clarendon, Oxford, 1961)
[2] S Chandrasekhar, *Astrophys. J.* **139**, 664 (1964)
[3] L Rayleigh, *Phil. Mag.* **32**, 529 (1916)
[4] H Bénard, *Ann. Chimie Phys.* **23**, 62 (1901)
[5] Å Nordlund and R F Stein, *Comp. Phys. Comm.* **59**, 119 (1990)
[6] R F Stein and Å Nordlund, *Astrophys. J.* **499**, 914 (1998)
[7] M Steffen, H-G Ludwig and B Freytag, *Astron. Nach. Supp.* **3**, 174 (2003)
[8] H H Plasket, *Mon. Not. R. Astron. Soc.* **114**, 251 (1954)
[9] M Asplund, N Grevesse and A J Sauval, in *Cosmic abundances as records of stellar evolution and nucleosynthesis* edited by T G Barnes, F N Bash, *ASP Conf. Ser.* **336**, 25 (2005)
[10] S Basu and H M Antia, *Phys. Rep.* **457**, 217 (2008)
[11] E Caffau, H-G Ludwig, M Steffen, B Freytag and P Bonifacio, *Solar Phys.* **268**, 255 (2011), arXiv:1003.1190
[12] M C Cross and P Hohenberg, *Rev. Mod. Phys.* **65**, 851 (1993)
[13] M C Begelman, R D Blandford and M J Rees, *Rev. Mod. Phys.* **56**, 255 (1984)
[14] J S Langer, *Rev. Mod. Phys.* **52**, 1 (1980)
[15] E N Parker, *Astrophys. J.* **145**, 811 (1966)
[16] S H Lubow and F Shu, *Astrophys. J.* **198**, 383 (1975)
[17] V M Canuto and I Mazzitelli, *Astrophys. J.* **370**, 295 (1991)
[18] S Basu and H M Antia, *J. Astrophys. Astron.* **15**, 143 (1994)
[19] P H Scherrer *et al*, *Solar Phys.* **162**, 129 (1995)
[20] J Schou, A G Kosovichev, P R Goode and W A Dziembowski, *Astrophys. J.* **489**, L197 (1997)
[21] H M Antia, *Astron. Astrophys.* **330**, 336 (1998)
[22] W H Press and S A Teukolsky, *Astrophys. J.* **213**, 183 (1977)
[23] A Fabian, J Pringle and M J Rees, *Mon. Not. R. Astron. Soc.* **172**, 15 (1975)
[24] J L Friedman, J R Ipser and L Parker, *Astrophys. J.* **304**, 115 (1986)
[25] D Lynden-Bell and J P Ostriker, *Mon. Not. R. Astron. Soc.* **136**, 293 (1967)
[26] M J Clement, *Astrophys. J.* **140**, 1045 (1964)

[27] D O Gough and M J Thompson, in *Solar interior and atmosphere* edited by A N Cox, W C Livingston and M Matthews, *Space Science Series* (University of Arizona Press) p. 519
[28] F Hill *et al*, *Science* **272**, 1292 (1996)
[29] A S Brun, H M Antia, S M Chitre and J-P Zahn, *Astron. Astrophys.* **391**, 725 (2002)
[30] M Asplund, N Grevesse, A J Sauval, C Allende Prieto and D Kiselman, *Astron. Astrophys.* **417**, 751 (2004); Erratum, *Astron. Astrophys.* **435**, 339 (2005)
[31] J N Bahcall and M H Pinsonneault, *Phys. Rev. Lett.* **92**, 121301 (2004)
[32] H M Antia and S Basu, *Astrophys. J.* **620**, L129 (2005)
[33] M H Ritzwoller and E M Lavely, *Astrophys. J.* **369**, 557 (1991)
[34] J Schou, J Christensen-Dalsgaard and M J Thompson, *Astrophys. J.* **433**, 389 (1994)
[35] E A Spiegel and J-P Zahn, *Astron. Astrophys.* **265**, 106 (1992)
[36] F P Pijpers, *Mon. Not. R. Astron. Soc.* **297**, L76 (1998)
[37] R H Dicke, J R Kuhn and K G Libbrecht, *Nature* **316**, 687 (1985)
[38] D O Gough and M J Thompson, *Mon. Not. R. Astron. Soc.* **242**, 25 (1990)
[39] H M Antia, S M Chitre and M J Thompson, *Astron. Astrophys.* **360**, 335 (2000)
[40] C S Baldner, H M Antia, S Basu and T P Larson, *Astrophys. J.* **705**, 1704 (2009)
[41] E M Lavely and M H Ritzwoller, *Phil. Tran. Phys. Sci. Eng.* **339**, 431 (1992)
[42] P Chatterjee and H M Antia, *Astrophys. J.* **707**, 208 (2009)